



Transcriptomic Analysis Reveals the Messenger RNAs Responsible for the Progression of Alcoholic Cirrhosis

Zhihong Yang,^{1*} Sen Han,^{1,2*} Ting Zhang,¹ Praveen Kusumanchi,¹ Nazmul Huda,¹ Kelsey Tyler,¹ Kristina Chandler,¹ Nicholas J. Skill,³ Wanzhu Tu,⁴ Mu Shan,⁴ Yanchao Jiang,¹ Jessica L. Maiers ,¹ Kristina Perez,¹ Jing Ma,¹ and Suthat Liangpunsakul ^{1,5,6}

Alcohol-associated liver disease is the leading cause of chronic liver disease. We hypothesized that the expression of specific coding genes is critical for the progression of alcoholic cirrhosis (AC) from compensated to decompensated states. For the discovery phase, we performed RNA sequencing analysis of 16 peripheral blood RNA samples, 4 healthy controls (HCs) and 12 patients with AC. The DEGs from the discovery cohort were validated by quantitative polymerase chain reaction in a separate cohort of 17 HCs and 48 patients with AC (17 Child-Pugh A, 16 Child-Pugh B, and 15 Child-Pugh C). We observed that the numbers of differentially expressed messenger RNAs (mRNAs) were more pronounced with worsening disease severity. Pathway analysis for differentially expressed genes for patients with Child-Pugh A demonstrated genes involved innate immune responses; those in Child-Pugh B belonged to genes related to oxidation and alternative splicing; those in Child-Pugh C related to methylation, acetylation, and alternative splicing. We found significant differences in the expression of heme oxygenase 1 (*HMOX1*) and ribonucleoprotein, PTB binding 1 (*RAVER1*) in peripheral blood of those who died during the follow-up when compared to those who survived. **Conclusion:** Unique mRNAs that may implicate disease progression in patients with AC were identified by using a transcriptomic approach. Future studies to confirm our results are needed, and comprehensive mechanistic studies on the implications of these genes in AC pathogenesis and progression should be further explored. (*Hepatology Communications* 2022;6:1361-1372).

Excessive alcohol consumption is the leading cause of several medical conditions, including alcohol-associated liver disease (ALD).⁽¹⁻³⁾ ALD comprises a spectrum of histopathological changes in patients with excessive alcohol consumption, ranging from alcoholic steatosis, steatohepatitis, advanced fibrosis, and cirrhosis.^(4,5) Alcoholic steatosis occurs in most if not all patients who consume alcohol excessively; however, progression of ALD to advanced stages, such as alcoholic cirrhosis (AC), only develops in 15%-20%

of excessive drinkers. Patients with compensated cirrhosis generally do not have signs or symptoms. However, the disease can progress into the decompensated state when patients develop complications from portal hypertension, such as ascites or variceal bleeding.⁽⁶⁾ At this stage, the overall prognosis and survival are poor.⁽⁷⁾

The pathogenesis of alcohol-induced liver injury is complex, involving alterations of lipid metabolism, oxidative stress, and the inflammatory signaling pathway.⁽⁸⁻¹⁰⁾ Several genetic components involved in

Abbreviations: AC, alcoholic cirrhosis; ALD, alcohol-associated liver disease; ARID4A, AT-rich interaction domain 4A; ATP5F1E, ATP synthase F1 subunit epsilon; ATP5MG, ATP synthase membrane subunit g; ATP5PO, ATP synthase peripheral stalk subunit OSCP; ATP6V0B, ATPase H+ transporting V0 subunit b; ATRX, ATRX chromatin remodeler; BATF2, basic leucine zipper ATF-like transcription factor 2; CAD, carbamoyl-phosphate synthetase 2, aspartate transcarbamylase, and dihydroorotase; CASP8AP2, caspase 8 associated protein 2; CENPF, centromere protein F; COL3A1, collagen type III alpha 1 chain; COX5B, cytochrome c oxidase subunit 5B; COX7A2L, cytochrome c oxidase subunit 7A2 like; COX7C, cytochrome c oxidase subunit 7C; CUL5, cullin 5; DDX60, DExD/H-box helicase 60; DECR1, 2,4-dienoyl-CoA reductase 1; DEGs, differentially expressed genes; DKC1, dyskerin pseudouridine synthase 1; DROSHA, Drosha ribonuclease III; EXO1, exonuclease 1; FAF2, Fas Associated Factor Family Member 2; FGF12, fibroblast growth factor 12; FGFR1, fibroblast growth factor receptor 1; FSTL1, follistatin like 1; GBP2, guanylate binding protein 2; GSEA, gene set enrichment analysis; HC, healthy controls; HLA-DRA, HLA class II histocompatibility antigen, DR alpha chain; HLA-DRB1, HLA class II histocompatibility antigen, DR beta 1; HMOX1, heme oxygenase 1; HSD17B13, hydroxysteroid 17-beta dehydrogenase 13; IFI35, interferon induced protein 35; IFI44L, interferon induced protein 44 like; IFIH1, interferon induced with helicase C domain 1; IFIT2, interferon induced protein with tetratricopeptide repeats 2; IRF1, interferon regulatory factor 1; JAG1, jagged canonical Notch ligand 1; JAG2, jagged canonical Notch ligand 2; KIF20B, kinesin family member 20B; KIF5B, kinesin family member 5B; LAP3, leucine aminopeptidase 3; LGALS3BP, galectin 3 binding protein; LPS, lipopolysaccharides; LRRC37A3, leucine-rich repeat-containing protein 37A3; MBOAT7, membrane bound O-acyltransferase domain containing 7; MELD, model for end-stage Liver Disease; MSX1,

these pathways are associated with susceptibility to ALD. Single-nucleotide polymorphisms of patatin-like phospholipase domain-containing protein 3 (*PNPLA3*), transmembrane 6 superfamily member 2

(*TM6SF2*), and membrane-bound O-acyltransferase domain-containing 7 (*MBOAT7*) lead to an increased risk of AC among heavy drinkers.^(11,12) Furthermore, two studies using genome-wide association and exome

msh homeobox 1; MYBL2, MYB proto-oncogene like 2; NDC80, NDC80 kinetochore complex component; NDUFA4, NDUFA4 mitochondrial complex associated; NDUFB5, NADH:ubiquinone oxidoreductase subunit B5; NDUFB7, NADH:ubiquinone oxidoreductase subunit B7; NQO2, N-ribosylidihydroquinone reductase 2; NR3C2, nuclear receptor subfamily 3 group C member 2; NRP1, neuropilin 1; NUMA1, nuclear mitotic apparatus protein 1; NUP98, nucleoporin 98; OAT, ornithine aminotransferase; OLR1, oxidized low density lipoprotein receptor 1; PAMPs, pathogen-associated molecular patterns; PAPLN, papilin, proteoglycan like sulfated glycoprotein; PARP14, poly(ADP-ribose) polymerase family member 14; PDGFA, platelet derived growth factor subunit A; PDK4, pyruvate dehydrogenase kinase 4; PF4, platelet factor 4; PGLYRP1, peptidoglycan recognition protein 1; PGLYRP4, peptidoglycan recognition protein 4; PLSCR1, phospholipid scramblase 1; PLS-DA, partial least squares discriminant analysis; PML, promyelocytic leukemia; PNPLA3, patatin-like phospholipase domain-containing protein 3; PPRC1, peroxisome proliferator-activated receptor gamma coactivator-related protein 1; RAVER1, ribonucleoprotein, PTB binding 1; RBM22, RNA binding motif protein 22; RPL41, ribosomal protein L41; S100A4, S100 calcium binding protein A4; SAMD9, sterile alpha motif domain containing 9; SAMD9L, sterile alpha motif domain containing 9 like; SERPINA5, serpin family A member 5; SGCD, sarcoglycan delta; SLC25A3, solute carrier family 25 member 3; SLC25A6, solute carrier family 25 member 6; SLC7A1, solute carrier family 7 member 1; SLCQ2A1, solute carrier organic anion transporter family member 2A1; STAG1, stromal antigen 1; STAT2, signal transducer and activator of transcription 2; STOX1, Storkhead Box 1; SUCLA2, succinate-CoA ligase ADP-forming beta subunit; TAP1, transporter 1, ATP binding cassette subfamily B member; TDRD7, tudor domain containing 7; THBD, thrombomodulin; TIMM13, translocase of inner mitochondrial membrane 13; TIMP1, TIMP metalloproteinase inhibitor 1; TM6SF2, transmembrane 6 superfamily member 2; TOP1, DNA topoisomerase I; TPR, translocated promoter region; TRIM26, tripartite motif containing 26; TRIM5, tripartite motif containing 5; TRRAP, transformation/transcription domain associated protein; UBE2L6, ubiquitin conjugating enzyme E2 L6; UPF1, UPF1 RNA helicase and ATPase; UQCRC1, ubiquinol-cytochrome c reductase, complex III subunit XI; UQCRCQ, ubiquinol-cytochrome c reductase complex III subunit VII; VAV2, vav guanine nucleotide exchange factor 2; VCAN, versican; VEGFA, vascular endothelial growth factor A; VTN, vitronectin; WRN, WRN RecQ like helicase; YTHDC1, YTH domain containing 1.

Received October 4, 2021; accepted December 17, 2021.

Additional Supporting Information may be found at onlinelibrary.wiley.com/doi/10.1002/hep4.1903/supinfo.

*These authors contributed equally to this work.

Supported by the National Institutes of Health (K01AA26385 to Z.Y., K01DK112915 to J.L.M.), Indiana University Research Support Fund (Grant IU RSFG to Z.Y.), Ralph W. and Grace M. Showalter Research (to Z.Y.), Indiana University School of Medicine Dean's Scholar in Medical Research (to S.L.), Indiana Institute for Medical Research (to Z.Y., P.K.), National Institute of Diabetes and Digestive and Kidney Diseases (R01 DK107682 to S.L.), National Institute on Alcohol Abuse and Alcoholism (R01 AA025208, R21AA024935, U01 AA026917, UH2/UH3 AA026903, U01AA026817 to S.L.), and Veterans Administration Merit Award (1I01CX000361 to S.L.).

© 2022 The Authors. *Hepatology Communications* published by Wiley Periodicals LLC on behalf of American Association for the Study of Liver Diseases. This is an open access article under the terms of the [Creative Commons Attribution-NonCommercial-NoDerivs](https://creativecommons.org/licenses/by-nc-nd/4.0/) License, which permits use and distribution in any medium, provided the original work is properly cited, the use is non-commercial and no modifications or adaptations are made.

View this article online at [wileyonlinelibrary.com](https://onlinelibrary.wiley.com).

DOI 10.1002/hep4.1903

Potential conflict of interest: Nothing to report.

ARTICLE INFORMATION:

From the ¹Division of Gastroenterology and Hepatology, Department of Medicine, Indiana University School of Medicine, Indianapolis, IN, USA; ²Key Laboratory of Carcinogenesis and Translational Research, Peking University Cancer Hospital, Beijing, China; ³Department of Surgery, Louisiana State University Health Science Center, New Orleans, LA, USA; ⁴Department of Biostatistics and Health Data Sciences, Indiana University School of Medicine, Indianapolis, IN, USA; ⁵Department of Biochemistry and Molecular Biology, Indiana University School of Medicine, Indianapolis, IN, USA; ⁶Roudebush Veterans Administration Medical Center, Indianapolis, IN, USA.

ADDRESS CORRESPONDENCE AND REPRINT REQUESTS TO:

Zhihong Yang, Ph.D.
Division of Gastroenterology and Hepatology
Department of Medicine
Indiana University School of Medicine
702 Rotary Circle
Indianapolis, IN 46202, USA
E-mail: yangjoe@iu.edu
Tel.: +1-317-988-4546
or

Suthat Liangpunsakul, M.D., M.P.H.
Division of Gastroenterology and Hepatology
Department of Medicine
Indiana University School of Medicine
702 Rotary Circle
Indianapolis, IN 46202, USA
E-mail: sliangpu@iu.edu
Tel.: +1-317-278-1630

sequencing identified a new locus at Fas-associated factor family member 2 (*FAF2*) and hydroxysteroid 17-beta dehydrogenase 13 (*HSD17B13*) associated with a reduced risk of cirrhosis.^(12,13) While these studies uncover underlying risk factors for ALD development and progression, our understanding of the mechanisms and what triggers the ALD progression are lacking.

Several lines of evidence illustrate that coding and noncoding RNAs play a crucial role in ALD pathogenesis.⁽¹⁴⁻¹⁸⁾ A comprehensive RNA analysis may elucidate underlying mechanisms in gene expression and pathways leading to ALD and disease progression. Transcriptomic profiling is a comprehensive way of measuring gene expression allowing the detection of differentially expressed genes (DEGs) and identification of the unannotated polymerase II RNAs.⁽¹⁹⁾ We hypothesized that the expression of specific coding genes is critical for the progression of AC from compensated to decompensated states. To test this hypothesis, global RNA profiling from peripheral blood RNA was performed in a well-characterized cohort of healthy controls (HCs) and patients with AC with different disease severity ranging from compensated to decompensated states. We determined the association of the unique set of peripheral blood messenger RNA (mRNA) expression with that in the liver of patients with AC and performed gene set enrichment analysis (GSEA) and functional protein association networks (STRING) to further understand the function of DEGs during the progression from compensated to decompensated states in patients with AC. Lastly, we determined the prognostic significance of this unique mRNA signature on the survival outcomes in patients with AC.

Participants and Methods

STUDY DESIGN AND HUMAN SUBJECT COHORT

HCs were recruited from outpatient clinics at the Roudebush Veterans Administration Medical Center (VAMC), Indianapolis, IN. Patients with AC were those who attended liver clinics at Indiana University Hospital or Roudebush VAMC. These patients had a history of alcohol consumption averaging at least 80 g/day (for men) or 50 g/day (for women) for at least 10 years. This criterion is based on epidemiological evidence of the relationship between alcohol

consumption and cirrhosis. The diagnosis of AC has been described.^(12,14,20,21) In brief, it was made using radiographic imaging, history of portal hypertension complications, or biopsy-proven cirrhosis, with the exclusion of other known causes of liver diseases, such as viral hepatitis B or C, autoimmune liver disease, hemochromatosis, or Wilson disease. The study was approved by the Institutional Review Board (IRB) at Indiana University–Purdue University Indianapolis (IUPUI) and Roudebush VAMC Research and Development Program. Written informed consent was obtained from each participant.

BASELINE DATA COLLECTION

Baseline demographics, clinical characteristics, and laboratory tests of the study cohort were obtained at the time of enrollment, as reported.⁽¹⁴⁾ Baseline Child-Pugh and Model for End-Stage Liver Disease (MELD) scores were calculated for patients with AC to further categorize them into compensated (Child-Pugh class A, AC1) and decompensated (Child-Pugh class B or C, relating to AC2 or AC3, respectively) liver diseases.

PERIPHERAL BLOOD COLLECTION AND RNA PROFILING

Peripheral blood was collected from venipuncture at enrollment into the PAXgene Blood RNA tube (Qiagen; catalog #762165). The sample was gently inverted and stored at -80°C within 2 hours of collection. Peripheral blood RNAs were extracted using a QIAamp RNA Blood Mini Kit (Qiagen, Hilden, Germany) according to the manufacturer's protocols. Blood RNAs from HCs ($n = 4$) and patients with AC ($n = 12$, with 4 patients for each Child-Pugh classification) were subjected to global transcriptomic profiling using the Arraystar human microarray, version 3.0 (Arraystar, Rockville, MD). The original raw data were uploaded to GitHub (https://github.com/yangjoe-iu/ALD_Blood-RNASeq). Quantitative polymerase chain reaction (qPCR) was used to validate the expression of mRNAs in a separate cohort of 17 HCs and 48 patients with AC. The baseline demographic and clinical characteristics are provided in Supporting Table S1. The primer's sequences are provided in Supporting Table S2.

HUMAN LIVER SPECIMENS

We also collected de-identified human liver specimens from a different cohort of patients with AC for mRNA analysis. The collection was performed under the IRB-approved protocol at the IUPUI.

BIOINFORMATIC ANALYSIS

The raw intensities of samples were grouped and uploaded to the online software (<https://www.metaboanalyst.ca/MetaboAnalyst/home.xhtml>) for the statistical analysis using algorithms they provided.⁽²²⁾ After the integrity check, the data were normalized by a pooled sample from HCs and logarithmically transformed. The partial least squares-discriminant analysis (PLS-DA) was performed using the *pls* function provided by the R *pls* package. Classification and cross-validation were conducted using the *caret* package. Differentially expressed mRNAs were identified through an adjusted *P* value of 0.05 and at least 2-fold differential gene expression to generate the volcano plot. The heat map and correlation analysis were generated using the default setting. Statistical analyses of differentially expressed mRNAs among HCs and patients with AC with different severities stratified by Child-Pugh classification were performed using one-way analysis of variance analysis (ANOVA).

GSEA was conducted using the GSEA software downloaded from <https://www.gsea-msigdb.org/gsea/index.jsp>. Raw intensities data were processed following the guidelines for RNA sequencing (RNA-Seq) data sets with GSEA.⁽²³⁾ Bubble plots were generated using the *ggplot2* package in R. Enrichment plots and heat maps were provided from the GSEA software. Functional protein association networks were analyzed using STRING (<https://string-db.org>). Venn diagrams were generated using the Venn Diagram package in R. The list of unique differential gene expression from each group was submitted to DAVID (<https://david.ncicrf.gov>) for the gene ontology terms and Kyoto Encyclopedia of Genes and Genomes pathway analysis. Bubble plots were generated by the R *ggplot2* package.

STATISTICAL ANALYSIS

We used descriptive statistics, such as mean, SEM, and frequencies (percentages). Statistical analysis was performed using a Student *t* test for unpaired data or ANOVA to determine the mean difference. We used

survival analyses to determine the prognostic significance of the selected mRNA transcripts and the survival outcome in subjects with AC. The survival analysis was conducted to determine the significance of the variable of interest and time to mortality as calculated by the date of enrollment until the time of death. Patients who survived were censored. Cox regression models were used to determine the hazard ratio (HR) and its 95% confidence interval (CI). The cut-off *P* value < 0.05 was considered statistically significant.

Results

TRANSCRIPTOMIC IDENTIFICATION OF DIFFERENTIALLY EXPRESSED PERIPHERAL BLOOD mRNAs IN HCs AND PATIENTS WITH AC

To identify genes differentially expressed during the progression of AC, we first performed transcriptomic profiling of peripheral blood obtained from HCs and patients with AC. Arraystar Human Microarray, version 3.0, was used for the global profiling of approximately 26,000 human protein-coding transcripts. We first analyzed the profiling in 16 peripheral blood RNA samples, 4 HCs, and 12 patients with AC. PLS-DA⁽²⁴⁾ illustrated two distinct clusters, suggesting the unique transcriptomic profiles in peripheral blood of patients with AC when compared to HCs (two-dimensional [2D] and 3D plots are shown in Supporting Fig. S1A,B). Using the cutoff of *P* < 0.05 and at least 2-fold differential gene expression, we identified 707 and 179 mRNAs that were up- and down-regulated, respectively, in patients with AC compared to HCs (Fig. 1A; Supporting Fig. S1C; Supporting Table S3). Genes with the most differential changes in their expression in AC compared to HCs are shown in Fig. 1A (bottom panel). Storkhead Box 1 (*STOX1*), sarcoglycan delta (*SGCD*), and cluster of differentiation 248 (*CD248*) were down-regulated, and major histocompatibility complex, class II, DR beta 1 (*HLA-DRB1*), peptidoglycan recognition protein 4 (*PGLYRP4*), and fibroblast growth factor 12 (*FGF12*) were up-regulated in patients with AC. Next, we normalized the raw data with mean values and used the Ward algorithm to generate a heat map of the top 25 (Fig. 1B), top 1,000 (Supporting Fig.

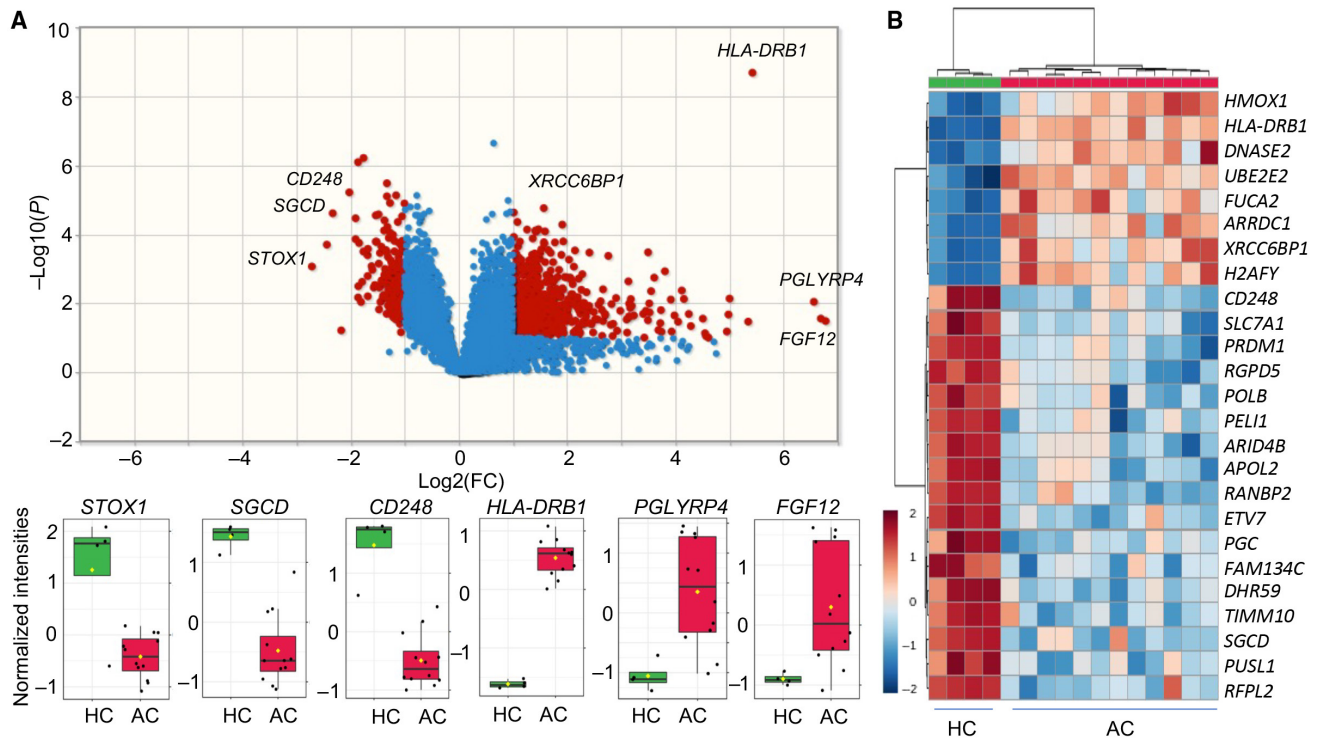


FIG. 1. Statistical analysis of differentially expressed mRNAs in peripheral blood of patients with AC. (A) Volcano plot displaying differentially expressed peripheral blood mRNAs in (B). Red dots represent significantly up-regulated (right) and down-regulated (left) mRNAs. Blue dots represent genes with no significant changes in gene expression (either $-2 > FC < 2$ or $P \geq 0.05$). Bottom panels show expression data of genes with the most significant changes in gene expression between HC (green boxes) and AC (red boxes) groups. (B) Heat map of the top 25 most significantly changed genes compared between HC and AC groups (HC, $n = 4$; AC, $n = 12$). Abbreviations: *STOX1*, storkhead box 1; *XRCC6BP1*, XRCC6 binding protein 1.

S1E), and top 50 (Supporting Fig. S1F) DEGs based on the P value. The correlation matrix also demonstrated two highly correlated gene groups with shared similar expression patterns according to the up- and down-regulated genes (Supporting Fig. S1D).

GSEA FOR DEGs IN PATIENTS WITH AC

GSEA was performed to gain an insight into the biological function of DEGs in patients with AC compared to those in HCs.⁽²³⁾ Within the 50 enriched gene sets, 13 and 37 gene sets were up- and down-regulated, respectively, in patients with AC (data not shown). Among the up-regulated gene sets, three gene sets were significantly enriched at the family-wise error rate at $P < 0.05$, including genes related to angiogenesis ($P = 0.009$), oxidative phosphorylation ($P = 0.026$), and xenobiotic metabolism ($P = 0.038$) (Fig. 2A). The selected enrichment score plots and the top 20 up-regulated enriched

genes are illustrated in Fig. 2C,E, respectively. Among the down-regulated gene sets, four gene sets were significantly enriched, including interferon- α (IFN- α) response ($P = 0.0001$), IFN- γ response ($P = 0.0001$), mitotic spindle ($P = 0.0001$), and G2M-checkpoint ($P = 0.0001$) (Fig. 2B). The selected enrichment score plots and top 20 down-regulated enriched genes are shown in Fig. 2D,F, respectively. Taken together, GSEA indicated the function of the up-regulated genes related to angiogenesis and metabolism while down-regulated genes were involved in IFN responses and cell-cycle pathways.

DIFFERENTIALLY EXPRESSED GENES IN PATIENTS WITH AC STRATIFIED BY DISEASE SEVERITY

We next explored the DEGs in peripheral blood of 12 patients with AC in our discovery cohort stratified by disease severity according to Child-Pugh

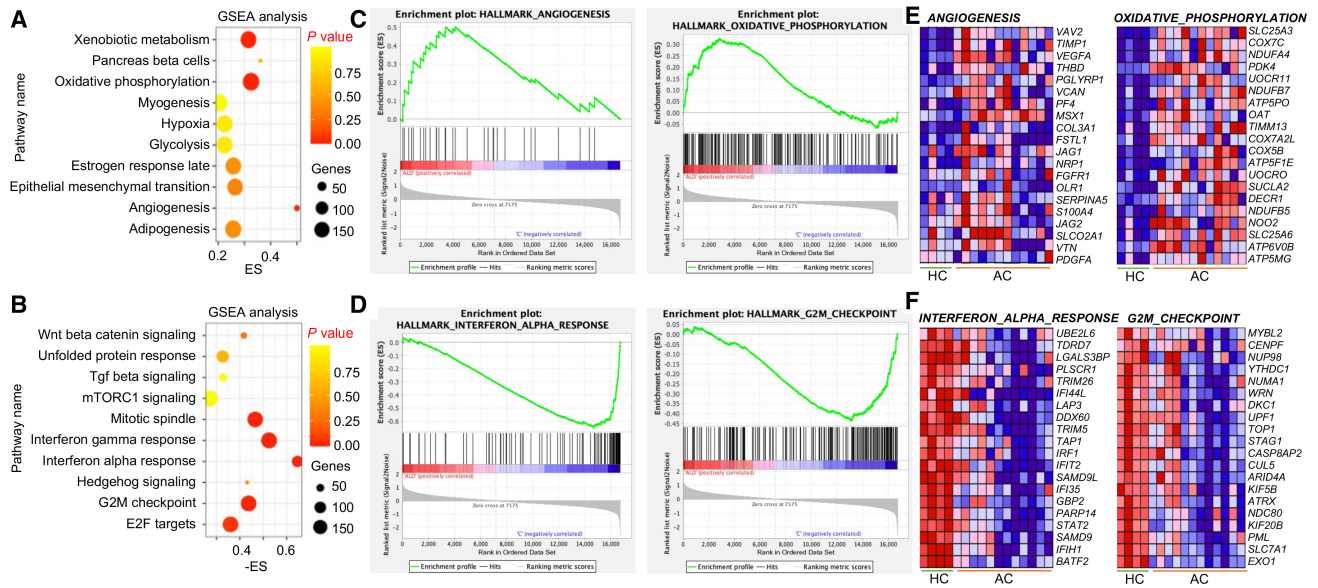


FIG. 2. GSEA of DEGs compared patients with AC to HCs. (A,B) Bubble plot of the selected top (A) 10 up- and (B) down-regulated gene sets in peripheral blood mRNA from patients with AC. The x axis represents the ES, and the size of the bubble represents the number of genes. Coloration from red to yellow represents the P value from low (red) to high (yellow). (C,D) ES plots for the indicated (C) up-regulated or (D) down-regulated gene sets. The green line is the running ES of the profile. The score at the peak indicates the ES score for that gene set. Vertical lines refer to individual genes and the position in a gene set. Coloration from red to blue represents the ranked gene list from up-regulated (red) to down-regulated (blue) genes in patients with AC compared to HCs. (E,F) Heat map of top 20 genes contributing to the enrichment of their respective pathway. A,C,E consist of analyses for the up-regulated gene sets, while B,D,F represent analyses for the down-regulated gene sets. Abbreviations: E2F, E2 transcription factor; ES, enrichment score; mTORC1, mammalian target of rapamycin complex 1; Tgf, transforming growth factor.

classification (4 patients for each Child-Pugh classification) compared to HCs (Fig. 3A). We observed that the number of differentially expressed peripheral blood mRNAs was more pronounced once disease severity worsened. Detailed analysis of these mRNAs in different Child-Pugh classes compared with HCs identified 142 and 164 mRNAs that were up- and down-regulated, respectively, in Child-Pugh class A patients compared to HCs, 581 up- and 270 down-regulated in Child-Pugh class B versus HCs, and 1,298 up- and 968 down-regulated in Child-Pugh class C versus HCs (Fig. 3B). PLS-DA demonstrated a unique gene expression profile in HCs and patients with AC with different severity (Fig. 3C). The top 25 most significantly DEGs among HCs and patients with AC with different Child-Pugh classification based on the fold change and P value are illustrated as a heat map (Fig. 3D) with the normalized reads of each gene in each group (Fig. 3E). *HLA-DRB1* was up-regulated in patients with AC regardless of disease severity when compared to HCs. The results were consistent with

those of Fig. 1B when we performed the analysis using samples from all patients with AC regardless of disease severity. The expression of ribosomal protein L41 (*RPL41*) and *HLA-DRA* progressively increased from compensated (Child-Pugh class A) to decompensated states (Child-Pugh class B and C) in patients with AC. The expression of papilin, proteoglycan like sulfated glycoprotein (*PAPLN*) was significantly up-regulated in patients with Child-Pugh class C compared to those in Child-Pugh class A and B (Fig. 3D,E). Expression of the genes pre-mRNA-splicing factor RNA binding motif protein 22 (*RBM22*), ribonucleoprotein, PTB binding 1 (*RAVER1*), nuclear receptor subfamily 3 group C member 2 (*NR3C2*), transformation/transcription domain-associated protein (*TRRAP*), peroxisome proliferator-activated receptor gamma coactivator-related protein 1 (*PPRC1*), leucine-rich repeat-containing protein 37A3 (*LRRRC37A3*), and translocated promoter region (*TPR*) was down-regulated during disease progression from Child-Pugh class A to class C (Fig. 3D,E).

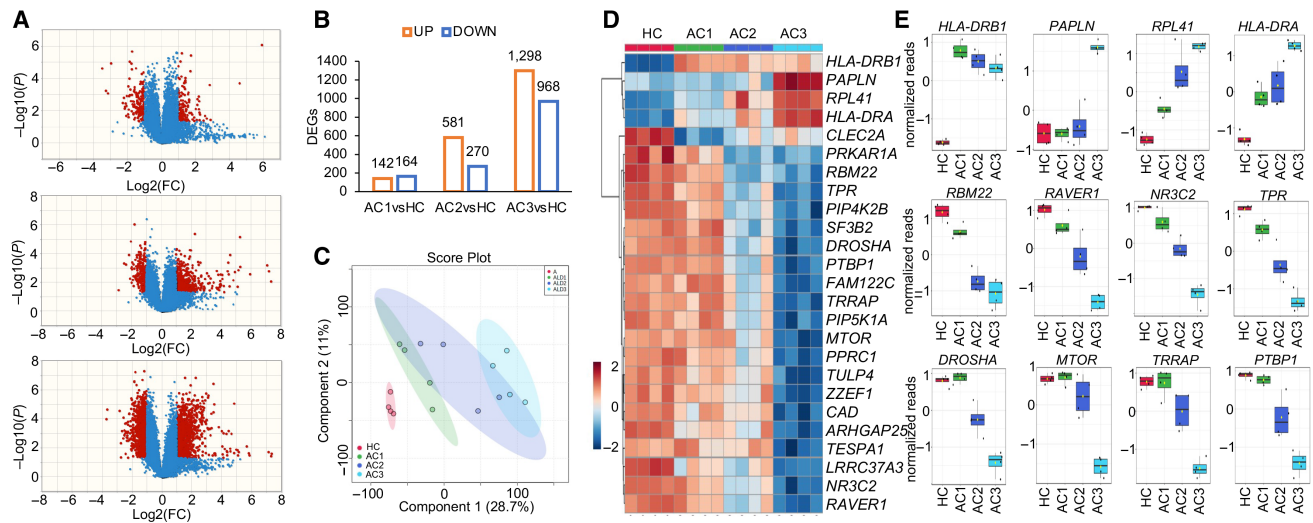


FIG. 3. DEG analysis in three study cohorts of human AC compared with HCs. The 12 human AC samples were divided into three groups based on the baseline Child-Pugh and MELD scores. (A) Volcano plots show DEGs for AC1 versus HCs (upper), AC2 versus HCs (middle), or AC3 versus HCs (bottom). (B) Graphic of the number of up-regulated or down-regulated genes. (C) Score plot of the PLS analysis of the samples from HC, AC1, AC2, and AC3. Each dot represents one sample. The highlighted ellipses represent the coverage of 95% of the subjects within each group. (D) Heat map of the top 25 most significantly changed genes based on P value ($n = 4/\text{group}$). (E) Normalized reads of selected genes in peripheral blood samples from different groups. Red boxes, HC; green boxes, AC1; blue boxes, AC2; light blue, AC3; $n = 4/\text{group}$. Abbreviations: *LRRC37A3*, leucine-rich repeat-containing protein 37A3; *PPRC1*, peroxisome proliferator-activated receptor gamma coactivator-related protein 1; *TRRAP*, transformation/transcription domain-associated protein; *RBM22*, RNA binding motif protein 22.

PATHWAY ANALYSIS BASED ON DEGs IN PATIENTS WITH AC DURING DISEASE PROGRESSION

To gain insight into pathways that may be involved during disease progression from compensated to decompensated states in patients with AC, we constructed a Venn diagram to determine the uniquely DEGs in peripheral blood for each Child-Pugh classification. We identified 104 DEGs in patients with AC regardless of disease severity (Fig. 4A). There were 98, 233, and 1,605 DEGs that were uniquely present in patients with AC with Child-Pugh class A, B, and C, respectively (Fig. 4A). Pathway analysis for DEGs specifically for patients with Child-Pugh class A demonstrated genes that are involved in inflammatory responses, including innate immunity and antiviral defense pathway (Fig. 4B). The DEGs in patients with Child-Pugh class B primarily belonged to pathways related to oxidation, hormone regulation, and alternative splicing (Fig. 4C). Lastly, those genes uniquely expressed in Child-Pugh class C were involved in isopeptide bond, ubiquitin conjugation, methylation, acetylation, phosphoprotein, and alternative splicing (Fig. 4D).

VALIDATION OF DEGs IN PERIPHERAL BLOOD OF PATIENTS WITH AC WITH DIFFERENT SEVERITY

Validation of DEGs in peripheral blood was performed in a separate cohort of 17 HCs and 48 patients with AC (17 Child-Pugh class A, 16 class B, and 15 class C; Supporting Table S1). We selected genes based on up- and down-regulated genes in heat map analysis (Fig. 1D). In addition, we also performed network analysis using STRING software (<https://string-db.org>; Supporting Fig. S2), and genes highlighted in functional enrichments in the network were selected. In total, 24 genes were selected for validation using qPCR analysis. We first performed the analysis using pooled samples from HCs and patients with AC with different severity (Supporting Fig. S3) to identify genes that were differentially expressed among groups for subsequent studies using an individual sample (as shown in each box in Supporting Fig. S3). Ten genes (*HLA-DRB1*, *HLA-DRA*, heme oxygenase 1 [*HMOX1*], *CD248*, *SGCD*, Drosha ribonuclease III

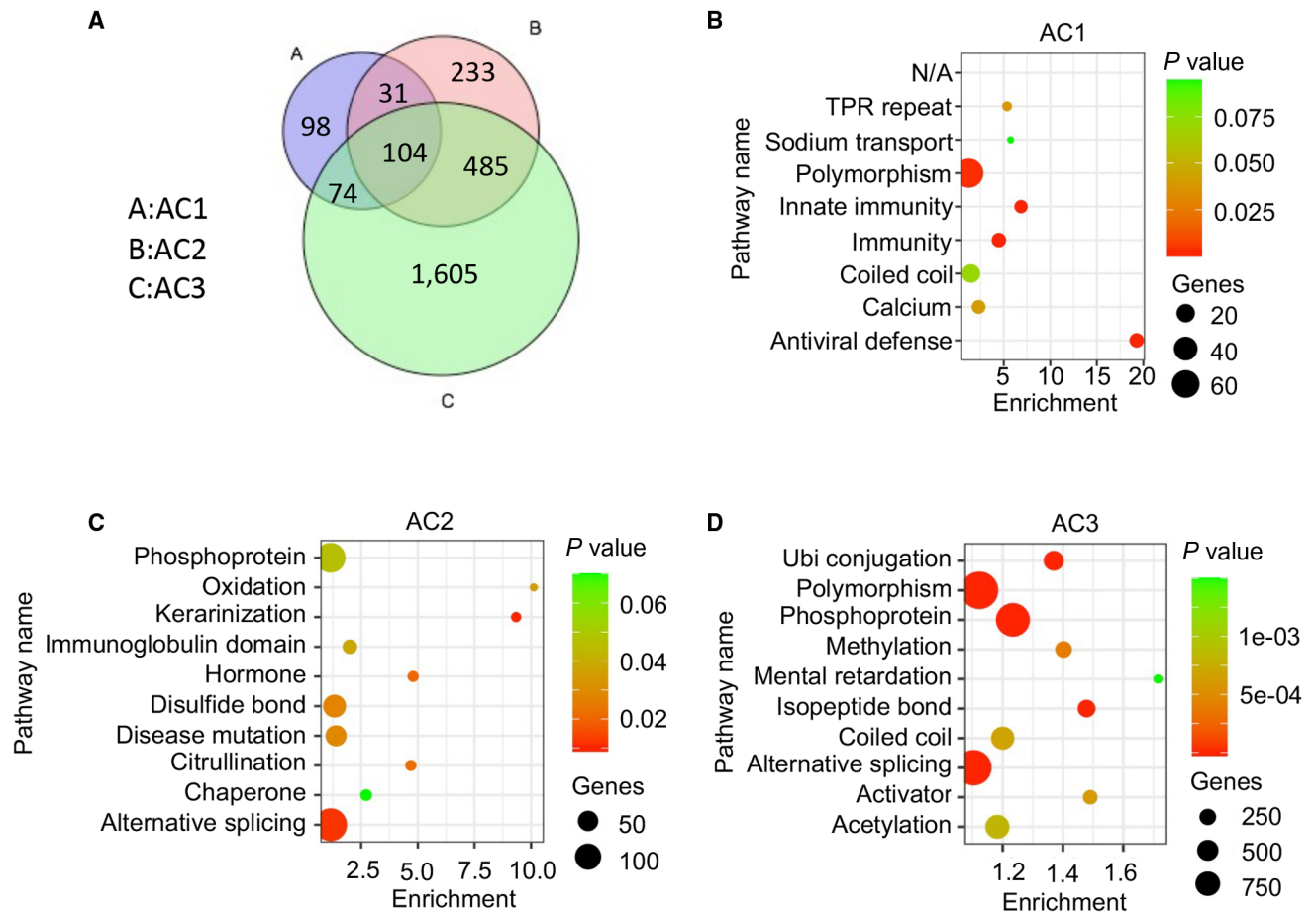


FIG. 4. Unique DEGs in each Child-Pugh class compared with HCs. (A) Venn diagram indicating the number of unique DEGs in each group and overlapping DEGs among groups. Blue circle, AC1 versus HCs; red circle, AC2 versus HCs; green circle, AC3 versus HCs. (B-D) Bubble plots of pathway analysis using DAVID (<https://david.ncifcrf.gov>) for unique DEGs in (B) AC1 versus HCs, (C) AC2 versus HCs, and (D) AC3 versus HCs. The x axis represents the enrichment score. Size of the bubble represents the numbers of genes in each pathway. Coloration from red to green represents the P value from low (red) to high (green). Abbreviations: N/A, not applicable; ubi, ubiquitin.

[*DROSHA*], polypyrimidine tract binding protein 1 [*PTBP1*], *RAVER1*, carbamoyl-phosphate synthase 2, aspartate transcarbamylase, and dihydroorotase [*CAD*], and *NR3C2*) were identified and validated in an individual sample (Fig. 5). There was a trend of increasing expression of *HLA-DRA* and *HLA-DRB1* in patients with AC compared to HCs. However, the difference was not statistically significant. The expression of *HMOX1* was progressively increased with worsening of AC from Child-Pugh class A to C. We also observed a significant reduction in the expression of *CD248* and *SGCD* in patients with AC compared to HCs. Consistent with RNA-Seq results, *DROSHA*, *PTBP1*, *CAD*, *RAVER1*, and *NR3C2* were

significantly reduced in patients with AC with different severity (Fig. 5).

COMPARISON OF DEGs IDENTIFIED IN PERIPHERAL BLOOD WITH THOSE IN THE LIVER OF PATIENTS WITH AC

Once ingested, alcohol, through its ability to distribute through body fluid compartments, can cause cellular injury in several organ systems. As the primary organ responsible for alcohol metabolism, the liver is a major organ that is affected by alcohol. We next asked if the differentially expressed mRNAs identified from

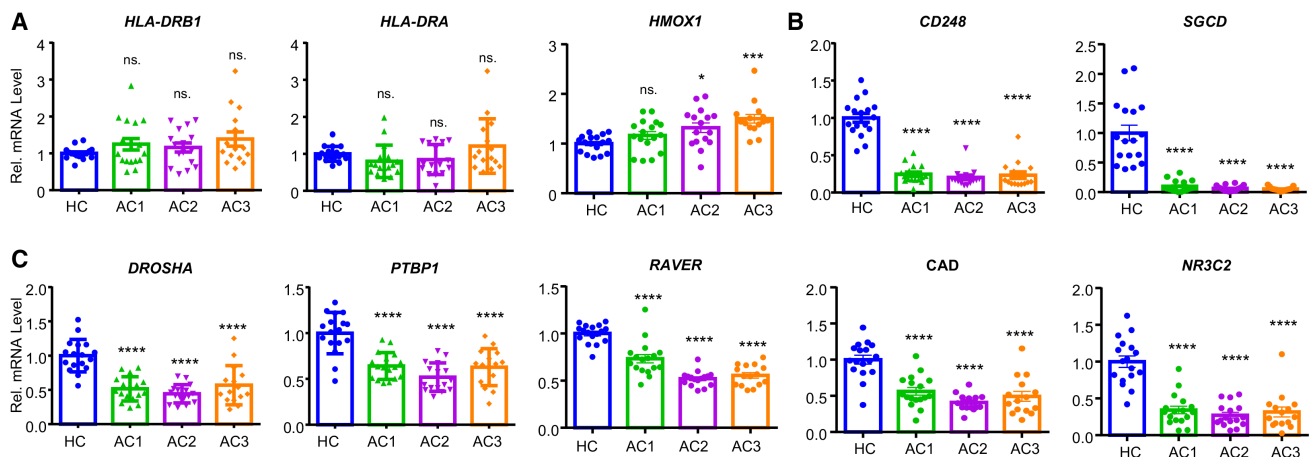


FIG. 5. Validation of selected genes in peripheral blood in HCs and ACs. (A–C) qPCR was used to detect selected DEGs in HCs (n = 17), AC1 (n = 17), AC2 (n = 16), and AC3 (n = 15). Each dot representing an individual sample. * $P < 0.05$, *** $P < 0.001$, **** $P < 0.0001$ versus HCs. Abbreviations: ns., not significant; Rel., relative.

peripheral blood in patients with AC (Figs. 1 and 5) have similar patterns in liver tissues. We examined the hepatic expression of each mRNA (Fig. 5) in liver tissues of another cohort of 8 HCs and 12 patients with AC. We observed a wide variability in the expression of each gene in the liver tissues of HCs and AC. Only expression of *HMOX1* and *PTBP1* was significantly reduced in the liver of patients with AC when compared to HCs (Fig. 6).

PROGNOSTIC SIGNIFICANCE OF SELECTED mRNA TRANSCRIPTS AND MORTALITY OUTCOMES IN PATIENTS WITH AC

During the median follow-up of 1.4 years, 14 patients died and 13 received a transplant among 48 patients with AC (Supporting Table S1). Baseline clinical characteristics and expression of selected mRNA transcripts for those who died and survived are shown in Supporting Table S4. Those who died had a significantly higher level of aspartate aminotransferase, total bilirubin, creatinine, MELD score, and *HMOX1*. However, the baseline level of serum albumin and *RAVER1* was significantly lower. Using the univariate COX proportional hazard model, we found that the expression of *HMOX1* (HR, 6.54; 95% CI, 1.19–35.7; $P = 0.03$) and *RAVER1* (HR, 0.006; 95% CI, 0–0.66; $P = 0.03$) in peripheral blood was associated with mortality during the follow-up (Supporting Table S5).

Discussion

Excessive alcohol consumption leads to adverse health outcomes affecting several organ systems. ALD represents a continuum of a disease process ranging from alcohol-induced hepatic steatosis, alcoholic hepatitis, advanced fibrosis, and cirrhosis.⁽¹⁾ The mechanisms of alcohol-induced liver injury are complex, involving crosstalk between organ systems. Alteration of several metabolic pathways is observed with ALD, including dysregulation of immune responses, impairment in hepatic regeneration, and epigenetic regulation,^(9,15,25) and all of these pathological processes are controlled by regulatory gene networks.^(16,26) Hepatic steatosis develops in most, if not all, excessive alcohol drinkers; however, advanced liver disease, such as AC, only occurs in a subset of patients. Patients with AC, in general, have clinical features similar to those with other chronic liver diseases. Liver tests are nearly normal in the compensated state, while complications from portal hypertension, such as ascites, hepatic encephalopathy, and esophageal varices, are common in decompensated patients. Once decompensation occurs, overall prognosis and long-term survival are poor. Expression of coding genes is altered in multiple pathways in ALD pathogenesis and during the disease progression, leading us to hypothesize that the expression of specific coding genes is critical for the progression of AC from compensated to decompensated states.

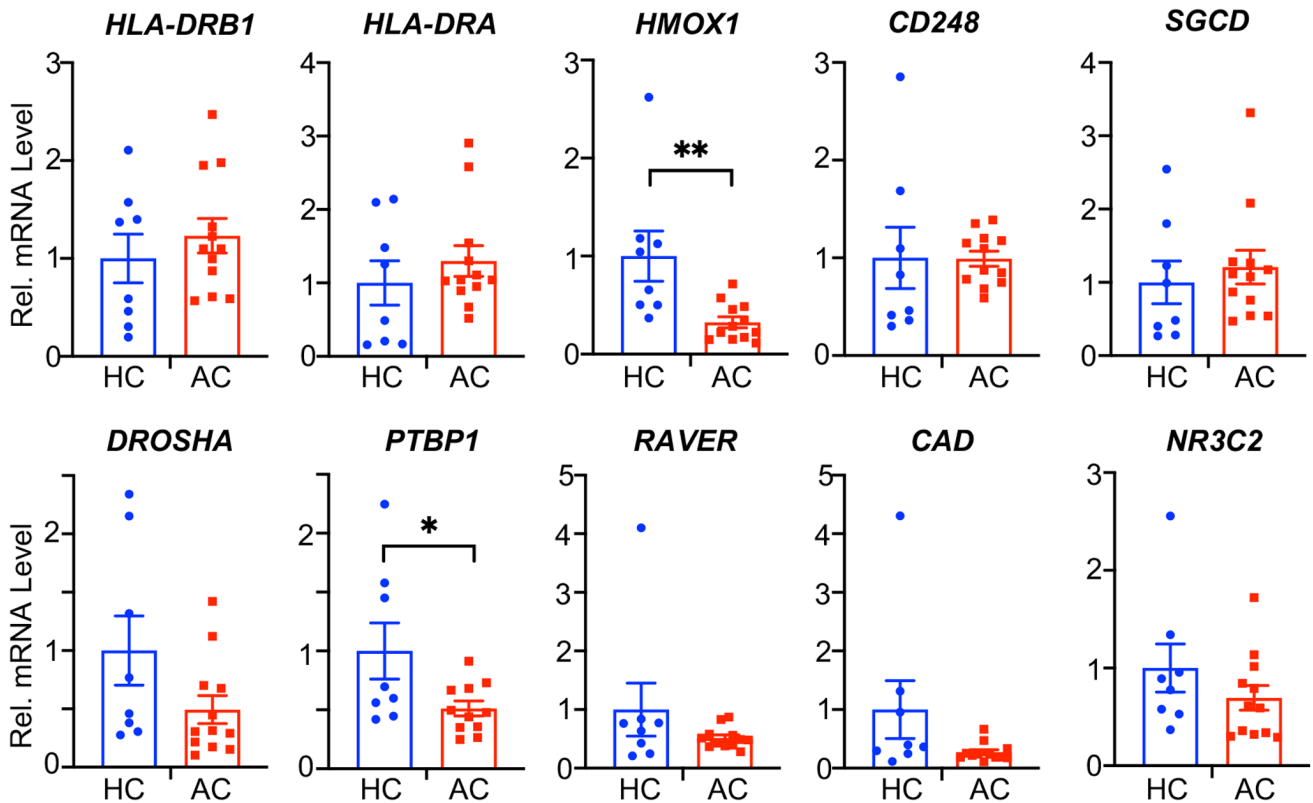


FIG. 6. Relative mRNA levels in HC and AC liver tissues. qPCR was used to detect selected genes in HCs (n = 8) and patients with AC (n = 12). * $P < 0.05$, ** $P < 0.01$, versus HCs. Each dot representing an individual sample.

Our results showed a unique peripheral blood RNA signature in patients with AC when compared to HCs. These differentially expressed mRNAs have distinct functions. We observed the genes related to angiogenesis as one of the top up-regulated gene sets. The formation of new vessels with the establishment of an abnormal angioarchitecture is a process related to progressive fibrogenesis and cirrhosis.⁽²⁷⁾ Additionally, several lines of evidence support a role for angiogenesis in the pathogenesis of portal hypertension.⁽²⁷⁾ Excessive alcohol use leads to an impairment of mitochondrial respiration secondary to lipid peroxidation products and inflammatory cytokines.⁽²⁸⁾ Together, they can affect mitochondrial permeability and thus impair oxidative phosphorylation,⁽²⁸⁾ as reflected by the induction of the gene sets related to this pathway in patients with AC. The observation on the induction of xenobiotic gene sets in AC is not surprising as the liver is known for its essential role in the processing of xenobiotics. Alteration in the liver architecture

secondary to cirrhosis leads to changes in the activity and level of drug-metabolizing enzymes, such as the cytochrome P450 gene family and glucuronidation capacity.^(21,29) A previous report demonstrated that peripheral blood mononuclear cells from patients with AC exhibited down-regulated IFN-stimulated gene expression, both constitutively and after an acute stimulus,⁽³⁰⁾ findings that are similar to our study. Lastly, α -tubulin is a major target for modification by highly reactive ethanol metabolites and reactive oxygen species.⁽³¹⁾ Alcohol also impairs the replication of normal hepatocytes at both the G1/S, and the G2/M transitions of the cell cycle.⁽³²⁾ These previous mechanistic studies likely underlie the observation in the alteration of the mitotic spindle and G2M-checkpoint gene sets in our patients with AC.

We carefully analyzed the function of the coding genes to gain a better insight into disease progression from compensated and decompensated states. As the severity of the disease worsens, we observed a higher

quantity of DEGs. We identified 10 genes from peripheral blood based on the fold-change, network analysis, and functional enrichments for validation; eight genes (*HMOX1*, *CD248*, *SGCD*, *DROSHA*, *PTBP1*, *RAVER1*, *CAD*, and *NR3C2*) are likely involved in disease progression from Child-Pugh class A to class C. Of these, we found (i) significant differences in the expression of *HMOX1* and *RAVER1* in peripheral blood of those who died during the follow-up when compared to those who survived and (ii) the expression level of these genes was associated with mortality in univariate COX analyses.

The *HMOX1* gene encodes for enzyme heme oxygenase; its function is to catalyze the reaction that degrades the heme group contained in hemoglobin, myoglobin, and cytochrome p450.^(33,34) *HMOX1* is ubiquitously expressed; its expression can be induced by pathogen-associated molecular patterns (PAMPs) and oxidative stress, two common mechanisms in the pathogenesis of ALD. Lipopolysaccharides (LPS) from gram-negative bacteria are representative of PAMP molecules. We previously reported a continuing increase in serum LPS level during disease progression from Child-Pugh class A to C in patients with AC⁽³⁵⁾; this is a plausible mechanism underlying our observation of an increase in *HMOX1* expression among patients with AC, as shown in the current study (Fig. 5). Moreover, induction of *HMOX1* may also represent an adaptive response against oxidative damage that is worsened during disease progression.⁽³⁶⁾

RAVER1, together with *PTB*, plays an important role in alternative splicing.⁽³⁷⁾ This is a process of selecting different combinations of splice sites within a messenger RNA precursor during RNA processing to produce variably spliced mRNAs.⁽³⁸⁾ We found the expression of *RAVER1* progressively decreased with worsening disease severity. How *RAVER1* and alterations in the RNA splicing process affect disease progression and mortality in patients with AC is not known and deserves further studies.

In the compensated state, alteration of the genes in peripheral blood primarily belongs to inflammatory responses and the innate immunity pathway. However, when the disease is shifted toward a decompensated state, we observed alterations of DEGs related to epigenetic regulation. MicroRNAs (miRNAs), as epigenetic modulators, affect the protein levels of the target mRNAs without modifying the gene sequence.⁽³⁹⁾ We recently reported changes in a unique miRNA

signature among patients with alcoholic hepatitis.⁽⁴⁰⁾ *DROSHA*, part of a multiprotein complex, is an upstream pathway of miRNA generation; it mediates the nuclear processing of the primary miRNAs into pre-miRNA.⁽⁴¹⁾ Mechanistic studies to determine the functional role of *DROSHA* in AC pathogenesis should be further explored.

We acknowledge several shortcomings of our study. First, the differential gene expression in peripheral blood may not reflect that in the liver, which is more aligned with the disease process in AC. To address this issue, we also examined the hepatic expression of each mRNA in the liver tissues of patients with AC. As expected, differential expression of genes in peripheral blood is not in the same direction as that in the liver. Second, because our analysis is performed in whole blood, it limits our ability to further explore the distribution of cell types that contribute to the differential expression we observed. Third, due to the nature of the study, we did not explore the underlying mechanism of how these genes are implicated in the pathogenesis of AC. Fourth, we did not capture data on the timing of last alcohol consumption before our transcriptomic analysis. Alteration in the gene expression and the potential contribution of lipid peroxidation products on oxidative dysfunction could depend on the duration of abstinence. Lastly, our sample size is relatively small, a future study to validate our results is needed.

In summary, we used a transcriptomic approach to identify unique mRNAs that may implicate disease progression in patients with AC. Future studies to confirm our results are needed, and comprehensive mechanistic studies on the implications of these genes in AC pathogenesis and progression should be further explored.

REFERENCES

- 1) Liangpunsakul S, Haber P, McCaughan GW. Alcoholic liver disease in Asia, Europe, and North America. *Gastroenterology* 2016;150:1786-1797.
- 2) Gilmore W, Chikritzhs T, Stockwell T, Jernigan D, Naimi T, Gilmore I. Alcohol: taking a population perspective. *Nat Rev Gastroenterol Hepatol* 2016;13:426-434.
- 3) Lachenmeier DW, Monakhova YB, Rehm J. Influence of unrecorded alcohol consumption on liver cirrhosis mortality. *World J Gastroenterol* 2014;20:7217-7222.
- 4) Sozio MS, Liangpunsakul S, Crabb D. The role of lipid metabolism in the pathogenesis of alcoholic and nonalcoholic hepatic steatosis. *Semin Liver Dis* 2010;30:378-390.

- 5) Mandrekar P, Bataller R, Tsukamoto H, Gao B. Alcoholic hepatitis: translational approaches to develop targeted therapies. *Hepatology* 2016;64:1343-1355.
- 6) Garcia-Tsao G, Abraldes JG, Berzigotti A, Bosch J. Portal hypertensive bleeding in cirrhosis: risk stratification, diagnosis, and management: 2016 practice guidance by the American Association for the Study of Liver Diseases. *Hepatology* 2017;65:310-335.
- 7) D'Amico G, Garcia-Tsao G, Pagliaro L. Natural history and prognostic indicators of survival in cirrhosis: a systematic review of 118 studies. *J Hepatol* 2006;44:217-231.
- 8) Udoh US, Valcin JA, Gamble KL, Bailey SM. The molecular circadian clock and alcohol-induced liver injury. *Biomolecules* 2015;5:2504-2537.
- 9) Gao B, Bataller R. Alcoholic liver disease: pathogenesis and new therapeutic targets. *Gastroenterology* 2011;141:1572-1585.
- 10) Gao B, Seki E, Brenner DA, Friedman S, Cohen JI, Nagy L, et al. Innate immunity in alcoholic liver disease. *Am J Physiol Gastrointest Liver Physiol* 2011;300:G516-G525.
- 11) Buch S, Stickelel F, Trepo E, Way M, Herrmann A, Nischalke HD, et al. A genome-wide association study confirms PNPLA3 and identifies TM6SF2 and MBOAT7 as risk loci for alcohol-related cirrhosis. *Nat Genet* 2015;47:1443-1448.
- 12) Schwantes-An TH, Darlay R, Mathurin P, Masson S, Liangpunsakul S, Mueller S, et al.; GenomALC Consortium. Genome-wide association study and meta-analysis on alcohol-related liver cirrhosis identifies novel genetic risk factors. *Hepatology* 2021;73:1920-1931.
- 13) Abul-Husn NS, Cheng X, Li AH, Xin Y, Schurmann C, Stevis P, et al. A protein-truncating HSD17B13 variant and protection from chronic liver disease. *N Engl J Med* 2018;378:1096-1106.
- 14) Yang Z, Ross RA, Zhao S, Tu W, Liangpunsakul S, Wang L. LncRNA AK054921 and AK128652 are potential serum biomarkers and predictors of patient survival with alcoholic cirrhosis. *Hepatol Commun* 2017;1:513-523.
- 15) Jiang Y, Zhang T, Kusumanchi P, Han S, Yang Z, Liangpunsakul S. Alcohol metabolizing enzymes, microsomal ethanol oxidizing system, cytochrome P450 2E1, catalase, and aldehyde dehydrogenase in alcohol-associated liver disease. *Biomedicines* 2020;8:50.
- 16) Zhang T, Yang Z, Kusumanchi P, Han S, Liangpunsakul S. Critical role of microRNA-21 in the pathogenesis of liver diseases. *Front Med (Lausanne)* 2020;7:7.
- 17) Yang Z, Zhang T, Han S, Kusumanchi P, Huda N, Jiang Y, et al. Long noncoding RNA H19 - a new player in the pathogenesis of liver diseases. *Transl Res* 2021;230:139-150.
- 18) Han S, Zhang T, Kusumanchi P, Huda N, Jiang Y, Yang Z, et al. Long non-coding RNAs in liver diseases: Focusing on nonalcoholic fatty liver disease, alcohol-related liver disease, and cholestatic liver disease. *Clin Mol Hepatol* 2020;26:705-714.
- 19) Papic N, Maxwell CI, Delker DA, Liu S, Heale BS, Hagedorn CH. RNA-sequencing analysis of 5' capped RNAs identifies many new differentially expressed genes in acute hepatitis C virus infection. *Viruses* 2012;4:581-612.
- 20) Whitfield JB, Masson S, Liangpunsakul S, Mueller S, Aithal GP, Eyer F, et al.; GenomALC Consortium. Obesity, diabetes, coffee, tea, and cannabis use alter risk for alcohol-related cirrhosis in 2 large cohorts of high-risk drinkers. *Am J Gastroenterol* 2021;116:106-115.
- 21) Yang Z, Kusumanchi P, Ross RA, Heathers L, Chandler K, Oshodi A, et al. Serum metabolomic profiling identifies key metabolic signatures associated with pathogenesis of alcoholic liver disease in humans. *Hepatol Commun* 2019;3:542-557.
- 22) Chong J, Wishart DS, Xia J. Using MetaboAnalyst 4.0 for comprehensive and integrative metabolomics data analysis. *Curr Protoc Bioinformatics* 2019;68:e86.
- 23) Subramanian A, Tamayo P, Mootha VK, Mukherjee S, Ebert BL, Gillette MA, et al. Gene set enrichment analysis: a knowledge-based approach for interpreting genome-wide expression profiles. *Proc Natl Acad Sci U S A* 2005;102:15545-15550.
- 24) Lee LC, Liang CY, Jemain AA. Partial least squares-discriminant analysis (PLS-DA) for classification of high-dimensional (HD) data: a review of contemporary practice strategies and knowledge gaps. *Analyst* 2018;143:3526-3539.
- 25) Gao B, Ahmad MF, Nagy LE, Tsukamoto H. Inflammatory pathways in alcoholic steatohepatitis. *J Hepatol* 2019;70:249-259.
- 26) Han S, Zhang T, Kusumanchi P, Huda N, Jiang Y, Liangpunsakul S, et al. Role of microRNA-7 in liver diseases: a comprehensive review of the mechanisms and therapeutic applications. *J Investig Med* 2020;68:1208-1216.
- 27) Fernandez M, Semela D, Bruix J, Colle I, Pinzani M, Bosch J. Angiogenesis in liver disease. *J Hepatol* 2009;50:604-620.
- 28) Mansouri A, Gattoliat CH, Asselah T. Mitochondrial dysfunction and signaling in chronic liver diseases. *Gastroenterology* 2018;155:629-647.
- 29) Elbekai RH, Korashy HM, El-Kadi AO. The effect of liver cirrhosis on the regulation and expression of drug metabolizing enzymes. *Curr Drug Metab* 2004;5:157-167.
- 30) Weiss E, Rautou P-E, Fasseu M, Giabicani M, de Chambrun M, Wan JH, et al. Type I interferon signaling in systemic immune cells from patients with alcoholic cirrhosis and its association with outcome. *J Hepatol* 2017;66:930-941.
- 31) Groebner JL, Tuma PL. The altered hepatic tubulin code in alcoholic liver disease. *Biomolecules* 2015;5:2140-2159.
- 32) Clemens DL. Effects of ethanol on hepatic cellular replication and cell cycle progression. *World J Gastroenterol* 2007;13:4955-4959.
- 33) Dunn LL, Midwinter RG, Ni J, Hamid HA, Parish CR, Stocker R. New insights into intracellular locations and functions of heme oxygenase-1. *Antioxid Redox Signal* 2014;20:1723-1742.
- 34) Sebastián VP, Salazar GA, Coronado-Arrázola I, Schultz BM, Vallejos OP, Berkowitz L, et al. Heme oxygenase-1 as a modulator of intestinal inflammation development and progression. *Front Immunol* 2018;9:1956.
- 35) Liangpunsakul S, Agarwal R. Altered circadian hemodynamic and renal function in cirrhosis. *Nephrol Dial Transplant* 2017;32:333-342.
- 36) Malaguarnera L, Madeddu R, Palio E, Arena N, Malaguarnera M. Heme oxygenase-1 levels and oxidative stress-related parameters in non-alcoholic fatty liver disease patients. *J Hepatol* 2005;42:585-591.
- 37) Rideau AP, Gooding C, Simpson PJ, Monie TP, Lorenz M, Hüttelmaier S, et al. A peptide motif in Raver1 mediates splicing repression by interaction with the PTB RRM2 domain. *Nat Struct Mol Biol* 2006;13:839-848.
- 38) **Wang Y, Liu J, Huang BO, Xu Y-M, Li J, Huang L-F, et al.** Mechanism of alternative splicing and its regulation. *Biomed Rep* 2015;3:152-158.
- 39) Yao Q, Chen Y, Zhou X. The roles of microRNAs in epigenetic regulation. *Curr Opin Chem Biol* 2019;51:11-17.
- 40) **Yang Z, Zhang T, Kusumanchi P, Tang Q, Sun Z, Radaeva S, et al.** Transcriptomic analysis reveals the microRNAs responsible for liver regeneration associated with mortality in alcohol-associated hepatitis. *Hepatology* 2021;74:2436-2451.
- 41) Lee Y, Ahn C, Han J, Choi H, Kim J, Yim J, et al. The nuclear RNase III Drosha initiates microRNA processing. *Nature* 2003;425:415-419.

Author names in bold designate shared co-first authorship.

Supporting Information

Additional Supporting Information may be found at onlinelibrary.wiley.com/doi/10.1002/hep4.1903/supinfo.